28/38 GHz Dual-band Dual-polarized Highly Isolated Antenna for 5G Phased Array Applications

Chenhao Chu[1#], Jianfeng Zhu[2$], Shaowei Liao[3*], Anding Zhu[1#], and Quan Xue[3*]

[#] *RF and Microwave Research Group, School of Electrical and Electronic Engineering, University College Dublin, Dublin, Ireland.*

[$] *Beijing Key Laboratory of Network System Architecture and Convergence, Beijing University of Posts and Telecommunications, Beijing, China.*

[*] *School of Electronic and Information Engineering, South China University of Technology, Guangzhou, China.*

[1#] *chenhao.chu@ucdconnect.ie*

[3*] *eeqxue@scut.edu.cn*

***Abstract* — This paper proposed a new dual-band dual-polarized array antenna operating at 28 GHz and 38 GHz for 5G communication applications. Three stacked patches are adopted to achieve the dual-band operation. The lower band from 27.48 to 28.50 GHz is achieved by using the lower large patch, which is couple-fed by the middle patch. While the upper band from 36.94 to 40.43 GHz is achieved by using the middle and upper patches. The two patches resonant at 38 and 40 GHz respectively and the two resonant modes coupled together, which greatly enhances the upper band. To increase the polarization isolation in the lower band, a shorting pin connecting the lower patch and ground is utilized. Taking advantages of the multi-layer technology, the position of the vertical feeding probe between the middle patch and lower patch is slightly shifted to ensure the good impedance matching in both lower band and upper band. For the antenna element, the simulated -12 dB bandwidths are 27.48-28.50 GHz and 36.94-40.43 GHz for the two bands, respectively. The in-band gains are over 6 dBi in the lower band, and over 4 dBi in the upper band. For the 2×2 antenna array, the isolations are better than 20 dB in both bands.**

Index Terms — 5G, Antenna-in-Package (AiP), dual-band, dual polarization, millimeter wave

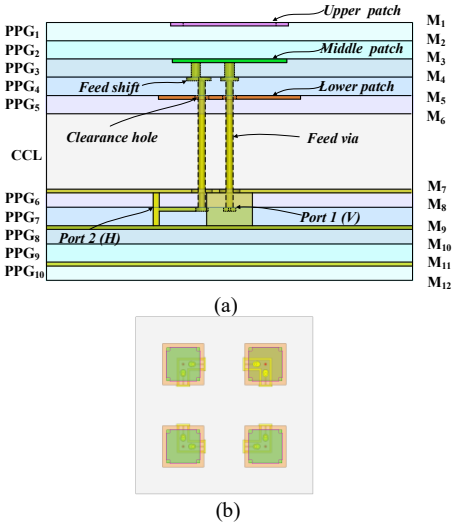

Fig. 1. (a) Stackup of the proposed AiP structure. (b) 2x2 antenna array package layout.

I. Introduction

Millimeter-wave (mm-Wave) technologies have been undergoing an unprecedented development with the rise of fifth generation (5G) communications [1][2]. Four different frequency bands around 28, 38, 60, and 73 GHz have been considered as mm-Wave candidates for both indoor and outdoor environments [3]. Among them, 28 and 38 GHz frequencies can be used when employing steerable directional antennas at base stations and mobile devices [4].

In mm-Wave design, it is popular to integrate the front-end circuit with the antenna in a cost-effective way. The antenna-in-package (AiP) solution has received great attention with the advantages of compactness, low cost, high reproducibility, and reliability [5]. Particularly, various antenna arrays have been demonstrated for the mm-wave band using high-temperature cofired ceramics (HTCC) [6], low temperature cofired ceramics (LTCC) [7], and high-density interconnect (HDI) [8] technologies using low-loss organic substrates.

In this work, a new dual-band dual-polarized array antenna operating at 28 GHz and 38 GHz for 5G communication applications using the HDI technique is proposed. For the antenna element, three stacked patches are adopted to achieve the dual-band performance. To increase the polarization isolation in the lower band, a shorting pin connecting the lower patch and ground is utilized. Taking advantages of the multi-layer technology, the position of the vertical feeding probe between the middle patch and lower patch is slightly shifted to ensure the good impedance matching in both lower band and upper band. A new π-shaped decoupling structure is utilized in the 2×2 array, improved the port isolation of the same polarization both in E-plane and H-plane.

II. Antenna in Package Structure

The antenna-in-package (AiP) layer stackup is illustrated in Fig. 1. Based on the HDI or surface laminate circuitry process, the AiP solution consists of three parts: the CCL layer in the center, five PPG layers above and five PPG layers bottom. For the core layer, the dielectric constant is 3.6 and the loss tangent is 0.0013. While for the PPG layer, the dielectric constant is 3.6 and the loss tangent is 0.007. The copper metal layers are embedded in the upper part of each substrate layer. The antenna element is realized from layer PPG1 to PPG7 together with the CCL layer. The CCL layer is much thicker than the PPG layer, which is good

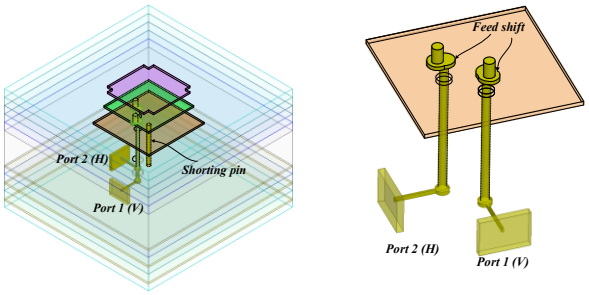

(a) (b)

Fig. 2. Dual-band dual-polarized antenna element. (a) 3D view of the proposed AiP structure. (b) Feed via and feed shift structure.

to achieve wider bandwidth at 28GHz. Though no structure is design on layer PPG8 and PPG9, the two layers are remained to ensure the manufacturing stability and reduce the manufacturing difficulty. Whereas layer PPG10 is for the phase shift feeding lines. In general, a symmetrical AiP structure is formed.

The 2x2 phased-array package concept is shown in Fig. 1 (b). The distance between the elements are adopted 4.65mm in both x- and y-direction, (0.44λ at 28 GHz) to achieve a wide scanning angle. However, the mutual coupling increases when the elements are placed close to each other. Therefore, a decoupling structure needs to be introduced.

III. Antenna Design and Simulation Results

A. Antenna Element

The 3D view of the dual-band dual-polarized phased array antenna element is shown in Fig .2. The height of lower patch from the antenna ground is large because of the thick CCL layer, which ensures the bandwidth at 28 GHz. During the design procedure, the positions of both lower patch and upper patch are changed several times. After tuning and optimization, middle patch is located on the PPG3 layer and upper patch is on the PPG1 layer, so that wide bandwidth can be achieved at 38 GHz. Four rectangles are cut on the corners of the upper patch, for a better impedance matching. However, there is always trade-off between the bandwidth in both bands with the traditional direct feed technique. Since the feed point can significantly change the impedance matching of microstrip patch antenna, a new feed shift structure is introduced in the AiP element design. For vertical polarization, the signals come from the feed line on PPG7. The feed via is connected to the feed line and pass the antenna ground through a hole. A clearance hole is dug on the lower patch so that the via can pass through and feed the lower patch by coupling. Feed shift is utilized to adjust feed point on the middle patch, while keeping that on the lower patch unchanged. For horizontal polarization, the structure is completely symmetrical along diagonal line. A shorting pin on the center connects the lower patch to the ground, which eliminates the higher-order modes current on the lower patch. It can enhance the polarization purity in lower band without deteriorating the performance of the upper band.

Figs. 3 (a) and (b) present the simulated return loss bandwidth and polarization isolation in both bands. The AiP element -12 dB return loss bandwidth is 27.48-28.50 GHz and 36.94-40.43 GHz. Meanwhile, from 27.0 to 28.35 GHz and from 40.0 to 40.5 GHz,

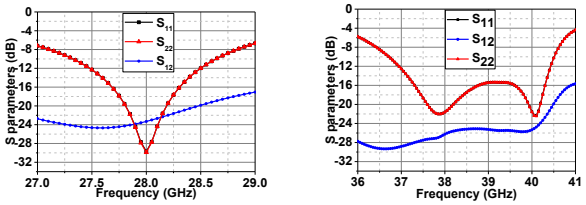

(a) (b)

Fig. 3. Simulated return loss bandwidth and polarization isolation for the AiP element. (a) Lower band. (b) Upper band.

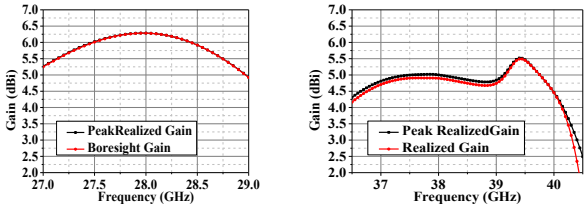

(a) (b)

Fig. 4. Simulated gain for the AiP element. (a) Lower band. (b) Upper band.

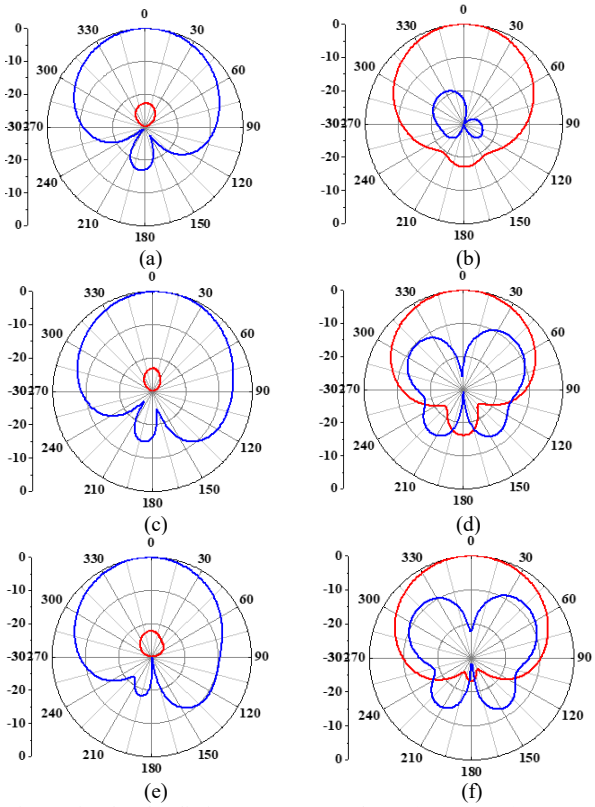

(a) (b) (c) (d) (e) (f)

Fig. 5. Simulated radiation pattern on E-plane (a) 28 GHz; (c) 38.5 GHz; (e) 40 GHz. Simulated radiation pattern on H-plane (b) 28 GHz; (d) 38.5 GHz; (f) 40 GHz.

the polarization isolations are lower than -20 dB. The extremely good design and simulated results ensure that the AiP element can perform well in spite of the fabrication errors and uncertainties, such as changes in the dielectric constant, metallization losses, and so on. Figs. 4 (a) and (b) show the simulated gain in both bands. The boresight gain is greater than 6 dBi from 27.5 GHz to 28.35 GHz, and greater than 4 dBi from 37 GHz to 40 GHz.

Fig. 5 illustrates the simulated radiation pattern on the E/H plane in both bands. Figs. 5 (a) and (b) show that in the lower band, the co-to-cross polarization is larger than 22.15 dBc and the gain at ±45° -angle is larger than 2 dBi. Figs. 5 (b), (c), (e) and

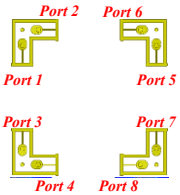

Fig. 6. Port distribution of 2x2 antenna array.

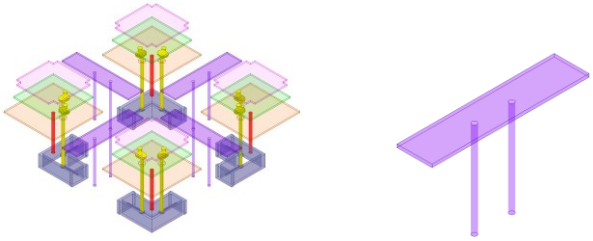

(a) (b)

Fig. 7. 2x2 antenna with symmetrical decoupling structure. (a) 3D view. (b) Single decoupling structure.

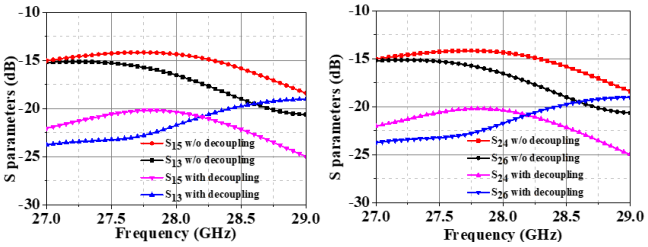

(a) (b)

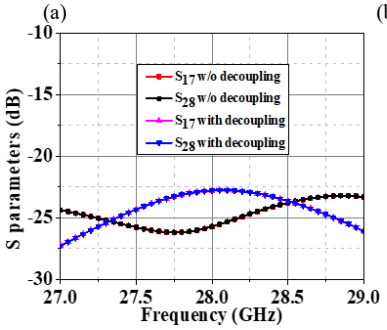

(c)

Fig. 8. Port isolation in the lower band without and with decoupling structure. (a) In the E-plane; (b) In the H-plane; (c) In the Diagonal plane.

(f) show that in the upper band, the co-to-cross polarization is larger than 23.52 dB and the gain at ±45° -angle is larger than 1 dBi.

B. Antenna Array

In order to improve the polarization purity and eliminate undesired sidelobes for the dual-band dual-polarized antenna array, the rotation symmetric technique is utilized. Fig. 6 demonstrates the port distribution of 2×2 antenna array. In this way, a wide scanning angle can be achieved when the ports are excited with different phase shift, ranging from 0° to 180°.

However, the port isolation is deteriorated due to the short distance between elements. To overcome this problem, a new π-shaped decoupling structure is introduced as shown in Fig. 7. It can decrease the coupling between the same polarization in both E-plane and H-plane. As shown in Fig. 8 and Fig. 9, the port isolation of the same polarization is enhanced about 5 dB in the lower band, while the isolation in the upper band remain lower than 20 dB.

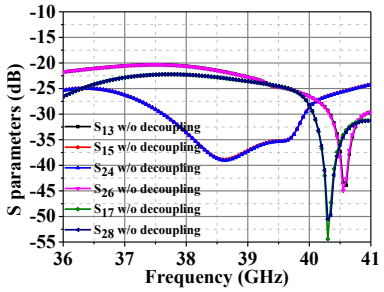

(a)

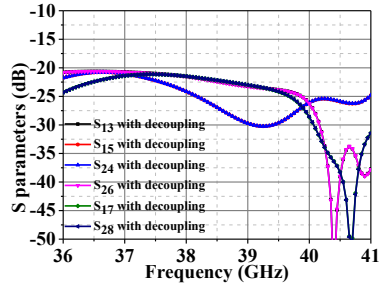

(b)

Fig. 9. Port isolation in the upper band. (a) Without decoupling structure. (b) With decoupling structure.

IV. Conclusion

A new dual-band dual-polarized antenna has been proposed. Stacked patch with feed shift structure is adopted to achieve the dual-band operation. For the antenna element, the simulated -12 dB bandwidths are 27.48-28.50 GHz and 36.94-40.43 GHz for the two bands, respectively. The in-band gains are over 6 dBi in the lower band, and over 4 dBi in the upper band. Additionally, the isolation between the vertical and horizontal polarization is lower than -20 dB. For the 2×2 antenna array, the element distance is 0.44λ at 28 GHz. With the new π-shaped decoupling structure, the simulated boresight gain reaches larger than 8.5 dBi and 10 dBi, respectively, for the two bands.

Acknowledgment

This work was supported by the Guangdong Innovative and Entrepreneurial Research Team Program (No. 2017ZT07X032).

References

[1] R. Daniels, J. Murdock, T. Rappaport, and R. Heath, "60 GHz wireless: Up close and personal," *IEEE Microwave Mag.*, vol. 11, no. 7, pp. 44–50, Jul. 2010.

[2] K.-C. Huang and D. J. Edwards, *Millimetre Wave Antennas for Gigabit Wireless Communications: A Practical Guide to Design and Analysis in a System Context*. Hoboken, NJ, USA: Wiley, 2008.

[3] K. Chandra, R. V. Prasad, B. Quang, I. G. M. M. Niemegeers, "CogCell: Cognitive interplay between 60 GHz picocells and 2.4/5 GHz hotspots in the 5G era", *IEEE Commun. Mag.*, vol. 53, no. 7, pp. 50-56, Jul. 2015.

[4] T. S. Rappaport et al., "Millimeter Wave Mobile Communications for 5G Cellular: It Will Work!," *IEEE Access*, vol. 1, pp. 335-349, 2013.

[5] A. Bisognin et al., "Noncollimating MMW Polyethylene Lens Mitigating Dual-Source Offset From a Tx/Rx WiGig Module," *IEEE Trans. Antennas Propag.*, vol. 63, no. 12, pp. 5908-5913, Dec. 2015.

[6] J. Lanteri et al., "60 GHz antennas in HTCC and glass technology," in *Proc. 4th Eur. Conf. Antennas Propag. (EuCAP'10)*, Barcelona, 2010, pp. 1-4.

[7] Y. P. Zhang, M. Sun, K. M. Chua, L. L. Wai, D. Liu, and B. P. Gaucher, "Antenna-in-Package in LTCC for 60-GHz radio," in *Proc. Int. Workshop Antenna Technol. Small Smart Antennas Metamater. Appl. (IWAT'07)*, 2007, pp. 279–282.

[8] R. Pilard et al., "HDI organic technology integrating built-in antennas dedicated to 60 GHz SiP solution," *Proc. IEEE Antennas Propag. Soc. Int. Symp. (APSURSI'12)*, Chicago, IL, 2012, pp. 1-2.